Journal of Applied Research and Technology

www.jart.icat.unam.mx

Journal of Applied Research and Technology 19 (2021) 140-152

Original

Superpixels extraction by an Intuitionistic fuzzy clustering algorithm

Dante Mújica-Vargas

Tecnológico Nacional de México/CENIDET, Cuernavaca, Morelos, México

Received 04 17 2020; accepted 02 15 2021
Available 04 30 2021

Abstract: A scheme to develop the image over-segmentation task is introduced in this paper, it considers the pixels of an image as intuitive fuzzy sets and develops an intuitionistic clustering process of them. In this regard, the main contribution is to provide a method for extracting superpixels with greater adherence to the edges of the regions. Experimental tests were developed considering biomedical grayscale and natural color images. The robustness and effectiveness of this proposal was verified by quantitative and qualitative results.

Keywords: superpixels extraction, intuitionistic fuzzy clustering, biomedical grayscale and natural color images

*Corresponding author.
E-mail address: dante.mv@cenidet.tecnm.mx (Dante Mújica-Vargas).
Peer Review under the responsibility of Universidad Nacional Autónoma de México.

1. Introduction

Superpixels are homogeneous regions of clustered pixels, taking into account low level features such as intensity, color, texture, spatial relationship, among others. They provide a simple, more compact and efficient representation of an image (Stutz et al., 2018). Some desired properties in the algorithms to extract superpixels are edge adhesion, precision and minimum runtime. To address this task, different approaches have been addressed in the state-of-art, e.g., those based on watersheds (Hu et al., 2015; Machairas et al., 2014; Neubert & Protzel, 2014), graph theory (Felzenszwalb & Huttenlocher, 2004; Humayun et al., 2015; Shi & Malik, 2000; Zhang et al., 2011), contour evolution (Buyssens et al., 2014), clustering (Achanta et al., 2010 Levinshtein et al., 2009; Li & Chen, 2015) and energy optimization (Yao et al., 2015). The simple linear iterative clustering (SLIC) algorithm is one of the most efficient for extracting superpixels (Achanta et al., 2010); however, like other methods, it has an insufficient spatial relationship, which can reduce the adhesion to the edges of the image as well as have an influence on the compactness and regularity of the superpixels.

Most of the aforementioned algorithms have outstanding performance; especially, when it comes to grayscale images. However, they require local or global features (texture, statistics, among others) to improve their performance. These algorithms are also sensitive to atypical information during the initialization stages and to the noise in the clustering stage; in addition, some of them require a parametric adjustment, processing steps or training phases. In contrast to these, in this paper, a proposal is given for extracting superpixels, which does not require a training stage; it works with only the intensity of the pixels or the color of the images as the only feature; and it does not require preprocessing to increase its performance. Beyond this, the only required parameter is the number of regions in which the image is oversegmented, although it makes a dynamic adjustment to obtain a correct number of superpixels depending on the size of the image.

The proposal consists of an adaptation of the intuitionistic fuzzy clustering algorithm engineered to extract superpixels, considering the properties of superpixels, such as the homogeneity of the segments as well as the adaptation to the natural limits of the image. The proposed approach considers pixels as intuitionist fuzzy sets; with this, each pixel belongs to all initial superpixels with different degrees of belonging. The homogeneity of the superpixels is refined in the clustering stage, in which the membership of each pixel for a certain superpixel is calculated iteratively. The labeling stage is done based on the membership matrix, which is obtained at the end of the clustering stage.

This paper is organized as follows: in Section 2, the relationship of intuitionist fuzzy numbers with image processing is described; in Section 3, the extraction of superpixels with the proposed algorithm is described in detail, for both grayscale and color images; in Section 4, the experimental configuration is indicated, in terms of the datasets used, metrics to quantify performance, and comparative methods; in Section 5, an analysis of the results obtained is shown; finally, conclusions and future work can be found in Section 6.

2. Intuitionistic fuzzy numbers applied on images

Let us X be a finite subset of the real p-dimensional vector space $\Re^p: X = \{x_1, x_2, \dots, x_n\} \subset \Re^p$; each $x_i = (x_{i1}, x_{i2}, \dots, x_{ip}) \subset \Re^p$ is the i-th pixel when the image is transformed into a column vector; and x_{ij} is the j-th pixel color space component of the pixel x_i; for most color spaces, it is satisfied that $1 < j < p = 3$. In order to express X as an intuitionistic fuzzy set $\Re^p: X^{IFS} = \{x_1^{IFS}, x_2^{IFS}, \dots, x_n^{IFS}\} \subset \Re^p$, each pixel can be fuzzified by (Atanassov, 2017; Chaira, 2015):

$$\mu(x_{ij}) = \frac{x_{ij} - \min(x_j)}{\max(x_j) - \min(x_j)} \tag{1}$$

where $\mu(x_{ij})$ is the membership degree, $\min(x_j)$ and $\max(x_j)$ are functions that allow to compute the minimum and maximum values of each color component, respectively. By using the Chaira intuitionistic fuzzy generator (Chaira, 2015), non-membership degree $\nu(x_{ij})$ can be computed based on the following expression:

$$\nu(x_{ij}) = \frac{1 - \mu(x_{ij})}{1 + (e^{\lambda} - 1) \cdot \mu(x_{ij})}, \quad \lambda \in [0,1] \tag{2}$$

where λ is a constant parameter. The hesitancy degree $\pi(x_{ij})$ can be determined from (1) and (2) as follows:

$$\pi(x_{ij}) = 1 - \mu(x_{ij}) - \nu(x_{ij}) \tag{3}$$

A formal definition of x_{ij}^{IFS} can be stated by means of the tuple:

$$x_{ij}^{IFS} = \left\{ \begin{matrix} \langle x_{ij}, \mu(x_{ij}), \nu(x_{ij}), \pi(x_{ij}) \rangle, & \forall x_{ij} \in X \\ | i = 1, \dots n \, | j = 1, \dots, p \end{matrix} \right\} \tag{4}$$

subject to the constraints a) $\mu(x_{ij}) + \nu(x_{ij}) + \pi(x_{ij}) = 1$ and b) $0 \leq \pi(x_{ij}) \leq 1$, for each $x_{ij} \in X$. In the context of image segmentation, there is the need to compute the similarity

between pixels; in this regard, the knowledge of a metric distance is required. Let us two pixels be expressed as intuitionistic fuzzy data $x_{1j}^{IFS} = \{\langle x_{1j}, \mu(x_{1j}), \nu(x_{1j}), \pi(x_{1j})\rangle\}$ and $x_{2j}^{IFS} = \{\langle x_{2j}, \mu(x_{2j}), \nu(x_{2j}), \pi(x_{2j})\rangle\}$, an euclidean intuitionistic fuzzy distance between them can be stated as (Szmidt, 2014):

$$\|x_{1j}^{IFS} - x_{2j}^{IFS}\|_2^2 = \left\{ \begin{matrix} \left(\mu(x_{1j}) - \mu(x_{2j})\right)^2 + \\ \left(\nu(x_{1j}) - \nu(x_{2j})\right)^2 + \\ \left(\pi(x_{1j}) - \pi(x_{2j})\right)^2 \end{matrix} \right\} \quad (5)$$

3. Superpixels extraction by an intuitionistic fuzzy clustering

3.1. Gray scale

To extract superpixels in grayscale images, an adaptation of the intuitionistic fuzzy C-means (IFCM) algorithm (Xu, 2013) is proposed. If each initial superpixel is considered to have representative data, then the objective function can be denoted as:

$$\mathcal{J}_m(X^{IFS}; U, V^{IFS}) = \sum_{j=1}^{N} \sum_{i=1}^{K} u_{ij}^m d^2\left(x_j, v_i\right) \quad (6)$$

where X^{IFS} are the pixels stated as intuitionist fuzzy sets, $V^{IFS} = \{V_1^{IFS}, V_2^{IFS}, \dots, V_K^{IFS}\}$ are the centroids of the K initial superpixels. These values are obtained by dividing the image into regular sized grids, with $R = \sqrt{N/K}$. To obtain a more accurate representation of the centroids V^{IFS}, the initialization process considers the local information of the initial superpixels, obtaining a more reliable representation. This initialization allows the proposed method to increase its performance and converge in a few iterations.

In this implementation, the search space is limited to a region of size $2R \times 2R$, in order to increase the speed of the algorithm and preserve the homogeneity of the segments. The conventional algorithm calculates the membership of a given data x_j, taking into account the centroids $V^{IFS} = \{V_1^{IFS}, V_2^{IFS}, \dots, V_K^{IFS}\}$. This may cause the segments not to be homogeneous because they are considered pixels that are not within the search space. To address this problem, the three closest centroids are considered, around the search space, as illustrated in Figure 1.

Expression to update the membership matrix is stated as follows:

$$u_{ij} = \frac{1}{\sum_{r=i}^{i \in K_p} \left(\frac{d^2\left(x_j^{IFS}, v_i^{IFS}\right)}{d^2\left(x_j^{IFS}, v_r^{IFS}\right)} \right)^{\frac{1}{m-1}}} \quad (7)$$

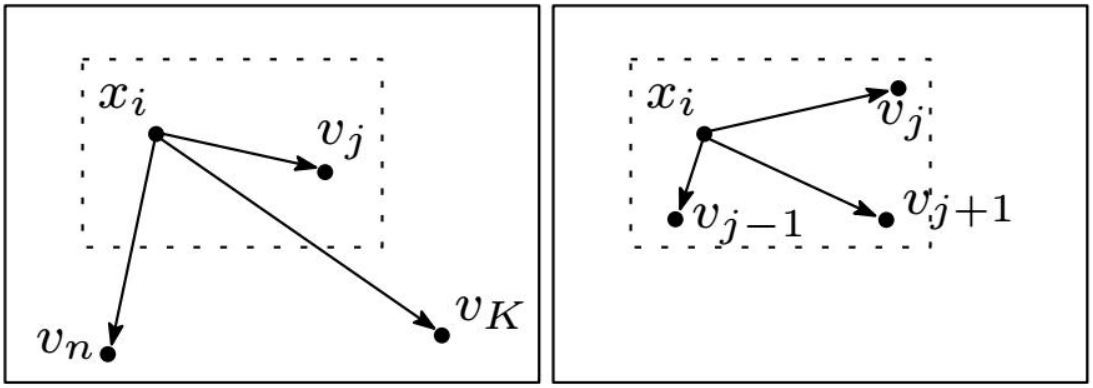

Figure 1. Search space reduction.

where u_{ij} is the membership, K_p is a vector with the three closest centroids $K_p \subset K$ and $d^2(x_j^{IFS}, v_i^{IFS})$ is the intuitionistic euclidean distance given by (5). The centroid vector update $V^{IFS} = \{V_1^{IFS}, V_2^{IFS}, \dots, V_K^{IFS}\}$ is done in a conventional way, using the following expressions

$$\mu(v_i) = \frac{\sum_{j=1}^{N} u_{ij}^m \mu(x_j)}{\sum_{j=1}^{N} u_{ij}^m}$$
$$\nu(v_i) = \frac{\sum_{j=1}^{N} u_{ij}^m \nu(x_j)}{\sum_{j=1}^{N} u_{ij}^m} \quad (8)$$
$$\pi(v_i) = \frac{\sum_{j=1}^{N} u_{ij}^m \pi(x_j)}{\sum_{j=1}^{N} u_{ij}^m}$$

where $v_i^{IFS}=(\mu(v_i), \nu(v_i), \pi(v_i))$ is the centroid, x_j is the datum to be clustered, u_{ij} is the membership degree of the j-th datum to j-th cluster and m the fuzzifier coefficient. This process is repeated until the error is smaller than an established threshold or the maximum number of iterations is reached. The accuracy of the algorithm can be controlled with variable ε. The maximum number of iterations is set to 10, although the preliminary tests of the algorithm are observed to converge between 2 and 5 iterations. On the basis of fuzzy clustering, each pixel belongs to all superpixels with a different membership degree. In view of this, the proposed approach obtains the highest membership degree. Based on this, the proposed approach obtains the highest membership degree u_{ij} of each pixel j and assigns it to label vector L^N by means of (9). Considering that the membership matrix $U = (u_{ij})_{N \times K}$ satisfies the constraint $\sum_{j=1}^{K} u_{ij} = 1$.

$$\begin{cases} L_j = arg\ max\ P(u_{ij}) \\ \{u_{ij} | u_{ij} \in U \wedge 1 \le i \le K, 1 \le j \le N,\ \forall ij\} \end{cases} \quad (9)$$

Subsequently, the oversegmentation is reinforced using a postprocessing step that links small superpixels with their neighbors. The union of the superpixels can be controlled through a parameter α; it is necessary to compute the average intensity s_k of the superpixels and the euclidean distance $d(s_k, s_{k+1}) < \alpha$ is satisfied.

Algorithm 1 summarizes the steps for the implementation of the proposed algorithm. The input is a grayscale image with size $W \times H$, where W and H are the width and height of the image. The number of superpixels K is also requested as input. In step 1, the image is transformed into a column vector; then, in step 2, the vector is taken to the intuitionistic fuzzy space by means of (1). V^{IFS} is initialized in step 3 (Algorithm 2), using the average value of the region, this process allows the region to be better represented since local information is taken into account. Before entering the iterative process, $u_{ij}^{(0)}$ is initialized in step 4. In step 6, the stop condition is stated. In step 7, the centroids are updated using the expressions (8). In steps 8-11, membership is calculated through the sliding on the regions. In steps 13-15, the superpixels of membership matrix U are extracted. The result is denoted as a label vector Y, which represents the oversegmented image.

Initialization

The IFCM algorithm can perform better with a good initialization of the centroids. The conventional algorithm uses a random initialization. In this proposal (algorithm 2), the arithmetic mean is used as the initialization form of the IFS in each initial region. The inputs are images represented as intuitionistic fuzzy sets X^{IFS} and number of superpixels K. The algorithm computes the arithmetic mean of each fuzzy index $(\bar{x}_\mu, \bar{x}_\nu \text{ and } \bar{x}_\pi)$ of pixels in the delimited region $2R \times 2R$. ϕ is a variable that ranges $0 < \phi < 1$, σ is a random number generated based on a Gaussian distribution.

3.2. Color

The proposed method can be extended to process color images, for this the three channels of the image must be included $I: W \times H \to \Re^3$. Each channel can be treated as an independent feature, so it is necessary to transform the input to the intuitionistic fuzzy domain by separating the channels. In this paper, the IJK color space is used since it is easy to convert; in addition to that, the IJK color space separates the brightness from channel I to the texture information in channels J and K. The conversion of the RGB color space to IJK is done with the following equations (Pătraşcu, 2007):

$$I = \frac{R+G+B}{3} \quad (10)$$

$$J = \frac{2R-G-B}{2\sqrt{3}} \quad (11)$$

$$K = \frac{G-B}{\sqrt{6}} \quad (12)$$

The proposed method for the color images is summarized in the algorithm 3. The algorithm does not have a significant change with respect to the version for grayscale images, since to process the three channels, they can be interpreted as independent vectors. In step 4, the expression is modified by adding x_j^{IFS}, which it is used to denote the channels, corresponding to the IJK color space, as intuitionistic fuzzy sets. These modifications can also be observed in the update of the centroid vector (step 7) and in the update of the membership matrix (step 11).

Algorithm 1: Grayscale SP-IFCA

input: Grayscale image X, number of superpixels K
output: Oversegmented image Y

$X \mapsto \tilde{X}$;
$\tilde{X} \mapsto X^{IFS}$;
Initialize $V_i^{IFS} = [\mu(v_i), \nu(v_i), \pi(v_i)]$; $i = 1, ..., K$; sampling pixels on the regular grid;
$u_{ij}^{(0)} \leftarrow \dfrac{1}{\sum_{r=1}^{K} \left(\dfrac{d^2(x_j^{IFS}, v_i^{IFS})}{d^2(x_j^{IFS}, v_r^{IFS})} \right)^{\frac{1}{m-1}}}$;
$l \leftarrow 0$;
while $max\ ||U^{(l+1)} - U^l|| < \varepsilon$ **do**
  $v_i^{IFS} \leftarrow \left\{ \dfrac{\sum_{j=1}^{N} u_{ij}^m \mu(x_j)}{\sum_{j=1}^{N} u_{ij}^m}, \dfrac{\sum_{j=1}^{N} u_{ij}^m \nu(x_j)}{\sum_{j=1}^{N} u_{ij}^m}, \dfrac{\sum_{j=1}^{N} u_{ij}^m \pi(x_j)}{\sum_{j=1}^{N} u_{ij}^m} \right\}$
  for $i \leftarrow 1$ **to** K **do**
    for each $x_j^{IFS} \in 2R \times 2R$ **do**
      if $\forall i, r,\ d^2(x_j^{IFS} - v_r^{IFS}) > 0$ **then**
        $u_{ij}^{(l)} \leftarrow \dfrac{1}{\sum_{i \in K_p} \sum_{r=i} \left(\dfrac{d^2(x_j^{IFS}, v_i^{IFS})}{d^2(x_j^{IFS}, v_r^{IFS})} \right)^{\frac{1}{m-1}}}$;
  $l \leftarrow l + 1$;
for $i \leftarrow 1$ **to** N **do**
  for $j \leftarrow 1$ **to** K **do**
    $Y_i \leftarrow \text{argmax}_j\ p(u_{ij} \in U : u_{ij} > Y_i)$;
return Y

Algorithm 2: Initialization

input: X^{IFS}, K.
output: V^{IFS}.

Set ϕ;
for $i \leftarrow 1$ **to** K **do**
  for $x_j^{IFS} \in 2R \times 2R$ **do**
    $\bar{x}_\mu \leftarrow \frac{1}{N_R} \sum_{j=1}^{N_R} \mu(x_j)$;
    $\bar{x}_\nu \leftarrow \frac{1}{N_R} \sum_{j=1}^{N_R} \nu(x_j)$;
    $\bar{x}_\pi \leftarrow \frac{1}{N_R} \sum_{j=1}^{N_R} \pi(x_j)$;
  for $x_j^{IFS} \in 2R \times 2R$ **do**
    $a_\mu \leftarrow max\{a_\mu, \mu(x_j) \in X^{FIS}\}$;
    $a_\nu \leftarrow max\{a_\nu, \nu(x_j) \in X^{FIS}\}$;
    $a_\pi \leftarrow max\{a_\pi, \pi(x_j) \in X^{FIS}\}$;
  $\mu(v_i) \leftarrow [(2a_\mu)\sigma - \phi] + \bar{x}_\mu$;
  $\nu(v_i) \leftarrow [(2a_\nu)\sigma - \phi] + \bar{x}_\nu$;
  $\pi(v_i) \leftarrow [(2a_\pi)\sigma - \phi] + \bar{x}_\pi$;
  $v_i^{IFS} \leftarrow \{\mu(v_i), \nu(v_i), \pi(v_i)\}$;
return V^{FIS}

Algorithm 3: Color SP-IFCA

input: Color image X, number of superpixels K
output: Oversegmented image Y

$X \mapsto \tilde{X}$;
$\tilde{X} \mapsto X^{IFS}$;
Initialize $V_i^{IFS} = [\mu(v_i), \nu(v_i), \pi(v_i)]$; $i = 1, ..., K$; sampling pixels on the regular grid ;
$u_{ij}^{(0)} \leftarrow \dfrac{1}{\sum_{r=1}^{K} \left(\dfrac{d^2(x_j^{IFS\times 3}, v_i^{IFS})}{d^2(x_j^{IFS\times 3}, v_r^{IFS})} \right)^{\frac{1}{m-1}}}$;
$l \leftarrow 0$;
while $max\ ||U^{(l+1)} - U^l|| < \varepsilon$ **do**
  $v_i^{IFS} \leftarrow \left\{ \dfrac{\sum_{j=1}^{N} u_{ij}^m \mu(x_j^3)}{\sum_{j=1}^{N} u_{ij}^m}, \dfrac{\sum_{j=1}^{N} u_{ij}^m \nu(x_j^3)}{\sum_{j=1}^{N} u_{ij}^m}, \dfrac{\sum_{j=1}^{N} u_{ij}^m \pi(x_j^3)}{\sum_{j=1}^{N} u_{ij}^m} \right\}$
  for $i \leftarrow 1$ **to** K **do**
    for each $x_j^{IFS\times 3} \in 2R \times 2R$ **do**
      if $\forall i, r,\ d^2(x_j^{IFS\times 3} - v_r^{IFS}) > 0$ **then**
        $u_{ij}^{(l)} \leftarrow \dfrac{1}{\sum_{r=i}^{i\in K_p} \left(\dfrac{d^2(x_j^{IFS\times 3}, v_i^{IFS})}{d^2(x_j^{IFS\times 3}, v_r^{IFS})} \right)^{\frac{1}{m-1}}}$;
  $l \leftarrow l + 1$;
for $i \leftarrow 1$ **to** N **do**
  for $j \leftarrow 1$ **to** K **do**
    $Y_i \leftarrow \text{argmax}_j\ p(u_{ij} \in U : u_{ij} > Y_i)$;
return Y

4. Experimental setup

4.1. Datasets

The performance of the proposed algorithm is evaluated against magnetic resonance imaging (MRI), for which a study was simulated in BrainWeb (Web, 2004); it was considered in $T1$ modality and corrupted with a density of 5% Gaussian noise. The study consists of 182 images with a size of 181×217 pixels. Additionally, the BSDS500 database was contemplated (Arbelaez et al., 2011), this is divided into a training subset of 200 images, 100 for validation and 200 testing images, all of them with sizes of 481×321 or 321×481 pixels.

4.2. Evaluation

In order to evaluate objectively the quality of the superpixels, the metrics boundary recall (BR) were considered (Martin et al., 2004), Error of subsegmentation (UE) (Achanta et al., 2010) and the variation explained (VE) (Moore et al., 2008). Runtime measured in seconds was also included, in order to know how fast the evaluated algorithms are in the superpixel extraction task.

Boundary recall is used to evaluate the adherence to the boundaries with respect to ground truth (Martin et al., 2004). This index can be computed by:

$$Rec(G,S) = \frac{TP(G,S)}{TP(G,S)+FN(G,S)} \tag{13}$$

where $FN(G,S)$ and $TP(G,S)$ are the number of $False - Positives$ and $True - Positives$, respectively; with respect to the boundaries given by an over segmentation obtained S and the ground truth G.

Error of subsegmentation describes the deviation of a superpixel with respect to a specific ground truth segment (Achanta et al., 2010), that is, it measures how each super pixel is superimposed with a ground truth segment.

$$UE = \frac{1}{N}\left[\sum_{l=1}^{M} \left(\sum_{s_j | s_j \cap g_i > B} |s_j| \right) - N \right] \tag{14}$$

where g_i is the segmentation ground truth and s_j the obtained superpixel. M represents the number of ground truth segments, N is the total number of pixels in the image and B is a minimum number of pixels that overlap g_i.

Variation explained measures the quality of a superpixel segmentation without using the ground truth segmentation (Moore et al., 2008), it is defined as:

$$EV = \frac{\sum_i(\mu_i-\mu)^2}{\sum_i(x_i-\mu)^2} \quad (15)$$

where x_i is the value of the real pixel, μ is global mean is the global average of pixels and μ_i is the average value of the pixels assigned to the super pixel that contains x_i.

4.3. Comparative algorithms

The performance of the proposed algorithm $SP-IFCA$ (superpixel extraction by an intuitionistic fuzzy clustering algorithm) is compared with W (watershed) (Hu et al., 2015), $SLIC$ (simple linear iterative clustering) (Achanta et al., 2010), LSC (linear spectral clustering) (Li & Chen, 2015), TP (turbopixel) (Levinshtein et al., 2009) and PB (pseudo-boolean superpixel) (Zhang et al., 2011) algorithms. These algorithms were considered because they can work with grayscale and color images, unlike others presented in the state of the art, which can only work with a specific type of images.

5. Experimental results

In these experiments the performance of the algorithms was evaluated before different number of superpixels; hence, it was assumed that the size of grid R depends on the total number of pixels in the image and the number of superpixels K required. To prevent the size of the grid range from being too small, the value of superpixels was bounded to $200 \leq K \leq 1450$ for the RMI gray scale and $200 \leq K \leq 6000$ for the color images. Therefore, the minimum interval size that is reached is $R = \sqrt{\frac{181*217}{1450}} = 5 \times 5$ and $R = \sqrt{\frac{481*321}{6000}} = 5 \times 5$, respectively. This ensures that the granularity of the superpixel is sufficient and that it contains the number of minimum pixels necessary to perform the calculations at the clustering stage.

5.1. Grayscale images: MRI of the brain

In this experiment, the algorithms developed the task of extracting superpixels from all images of the simulated MRI study. In Figure 2, the average performance against different number of superpixels K Is depicted.

Specifically, in terms of the level of adhesion to the edges (Figure 2a), a superior performance of the proposed method ($SP-IFCA$) can be observed in all number of superpixels considered. W and $SLIC$ show similar performance even though they use different approaches to generate superpixels, both outperform the other comparative algorithms from $K \geq 1000$. LSC produces good results up to $K \leq 1000$ but its yield tends to decrease from this value. TP reaches its best performance in $K = 800$, while PB has the lowest performance but with an upward improvement. In terms of the UE metric (Figure 2b), it can be seen that the proposed method obtained the minimum subsegmentation error in the range of $350 \leq K \leq 1450$, LSC has the best performance in $200 \leq K \leq 300$; however, from $K = 350$ its error has a growing behavior, $SLIC$ shows a linear trend just like $SP-IFCA$, TP tends to decrease in $200 \leq K \leq 600$ and to increase in $1000 \leq K \leq 1450$, W and TP present greater error, although their behavior decreases.

Figure 2c shows the level of adherence to the edges of the image, the highest value for all K values was obtained by $SP-IFCA$, followed by $SLIC$, LSC showed a decreasing behavior and the worst result in $850 \leq K \leq 1450$, PB presented the lowest values in $200 \leq K \leq 800$. Figure 2d reveals a similar trend in the processing time of most algorithms, which is interpreted as a proportional increase between the execution time and the number of superpixels. It highlights the proposed method $SP-IFCA$ with the shortest processing time ($0.005 \leq Runtime \leq 0.073$ seconds), followed by the SLIC algorithm, and so on. Instead, the TP algorithm required the longest processing time ($0.020 \leq Runtime \leq 0.251$ seconds).

In Figure 3, different representations of $K = 800$ superpixels are shown. In the form of contours (first row), as the average intensity of the segments (second row), was well comparison of the extracted segments with respect to ground-truth for Rec and UE metrics, in the third and fourth row, respectively. Given the amount of superpixels, the representation of the average intensity is not very supportive since it shows similar results. On the other hand, the representation of contours exposes the W, LSC and $SP-IFCA$ algorithms as those that generate irregular superpixels with better adaptation to the edges, and therefore, a better preservation of details. The other two representations make it possible to highlight the superpixels that fail to adapt correctly (regions in red). With this representation it can be seen that $SP-IFCA$ has the best performance with respect to the ground truth segments for both Rec and UE metrics.

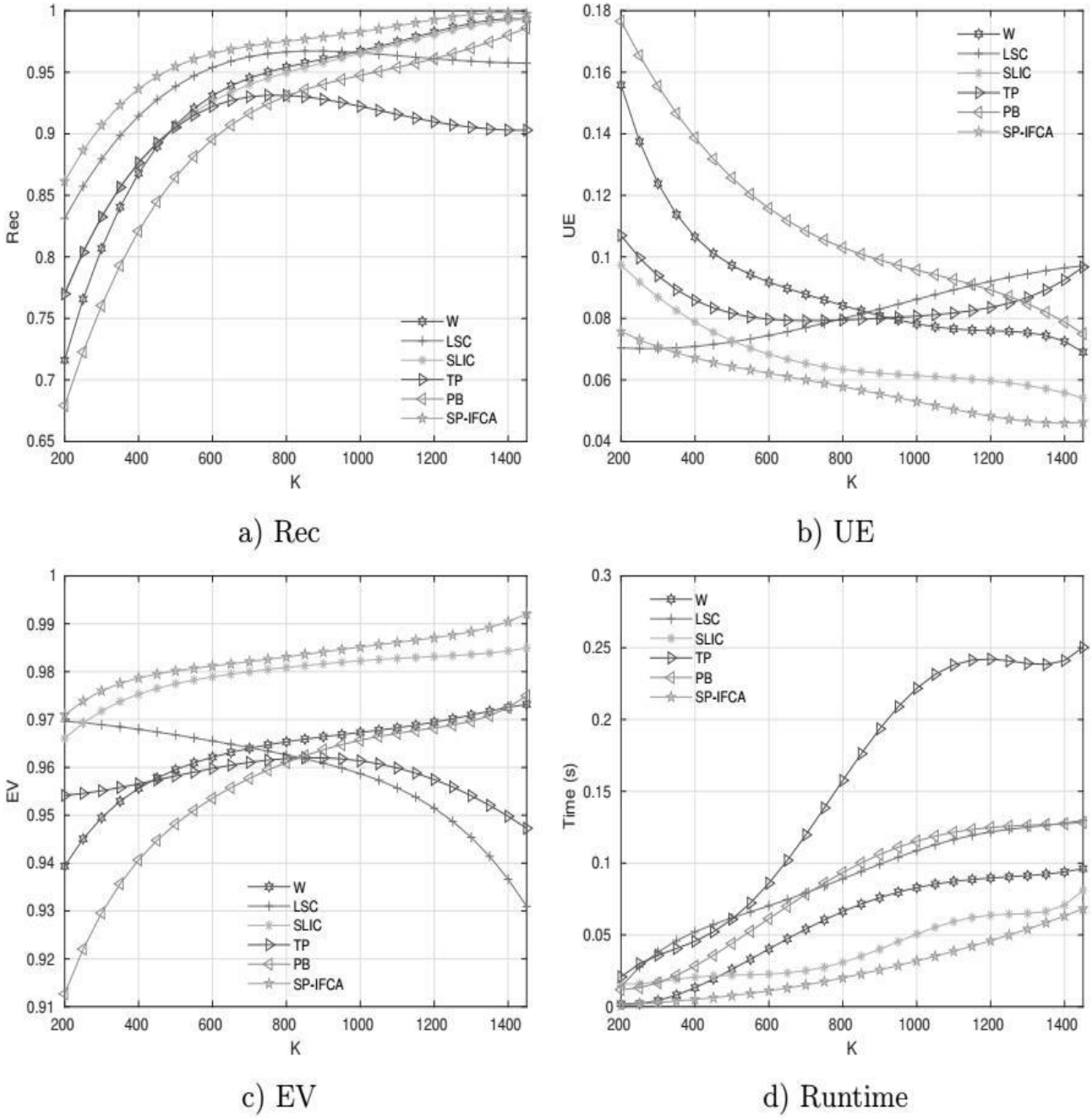

Figure 2. Average evaluation of the metrics, per MRI study and for different K values.

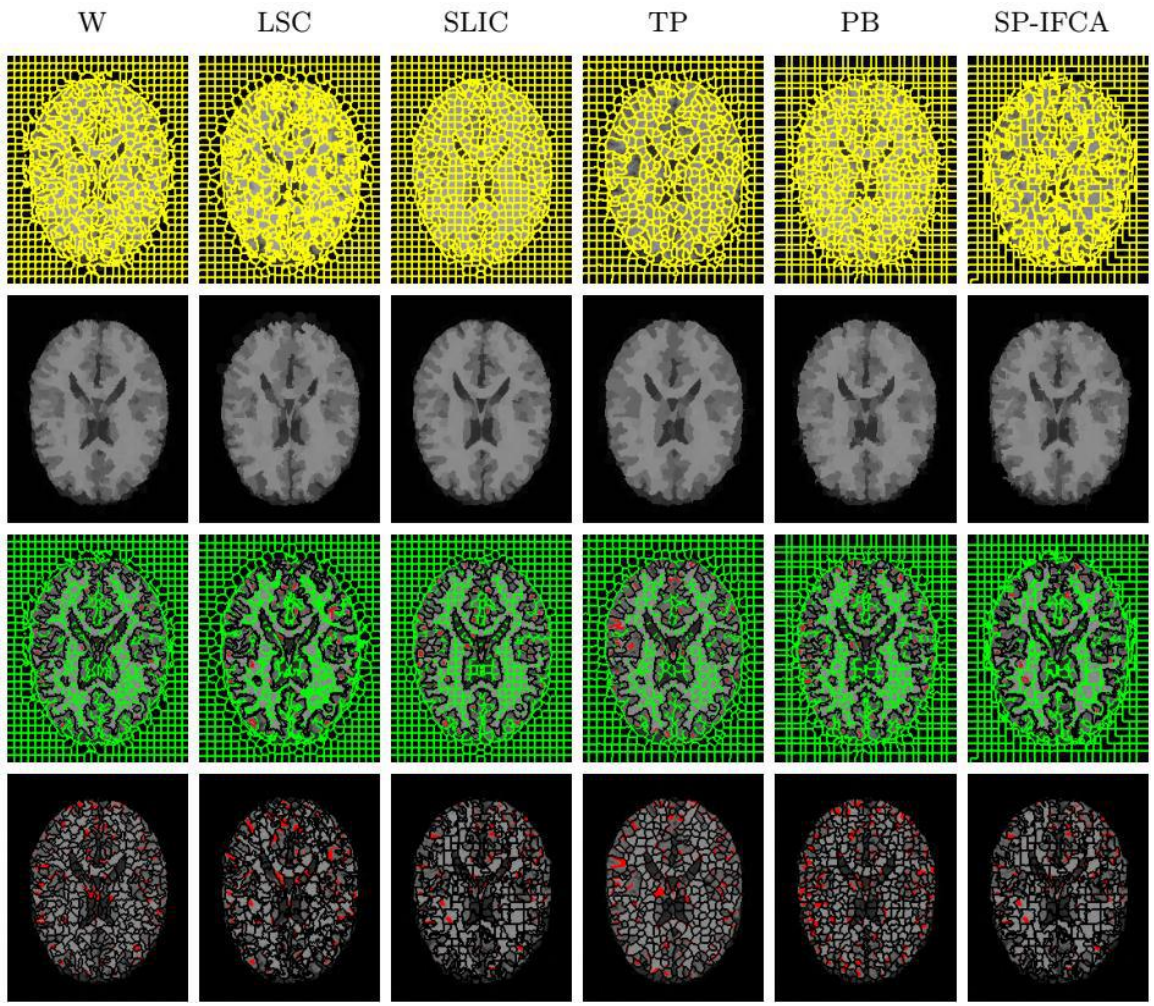

Figure 3. Visual results for the slice **90** of the simulated BrainWeb study with **5%** of noise density and $\boldsymbol{K = 800}$.

5.2. Color images: BSDS500

For the second experiment, the test subset of the database BSDS500 was used; the number of superpixels considered was in the range $200 \leq K \leq 6000$. The results obtained with respect to the Rec, UE and EV metrics are plotted in Figure 4. Adherence to limits is illustrated in Figure 4a, it is possible to see the best performance of $SP - IFCA$ algorithm for all K values, followed by LSC, the remaining algorithms present an ascending behavior as K is greater. The subsegmentation error can be seen in Figure 4b, the best performance of $SP - IFCA$ is ratified with a range of values $0.07 \leq UE \leq 0.157$, which decreases as the number of K increases, the other algorithms have the same decreasing trend, although with a greater error. The level of adhesion to the edges is shown in Figure 4c, the results of EV suggest that the best performance is that of $SP - IFCA$, followed by LSC and TP, $SLIC$ stands out from $K \geq 4300$; the other algorithms have lower performance.

On the other hand, the graphical trend of the processing time illustrated in Figure 4d confirms the increase in the processing time of all the algorithms, when it comes to color images; which is obvious since in this case three information channels are being processed. It can be seen that for $K \geq 250$ superpixels, the proposed method required the least processing time, i.e., $0.075 \leq Runtime \leq 0.166$ seconds. The rest of the algorithms showed good performance in terms of processing time.

To exemplify the extraction of superpixels in their different representations, image 230063 was oversegmented in $K = 800$ superpixels (Figure 5). A smaller amount of regions in red color can be observed by the proposed $SP - IFCA$ algorithm, which implies a better adaptation of the extracted superpixels compared to those suggested in the ground truth.

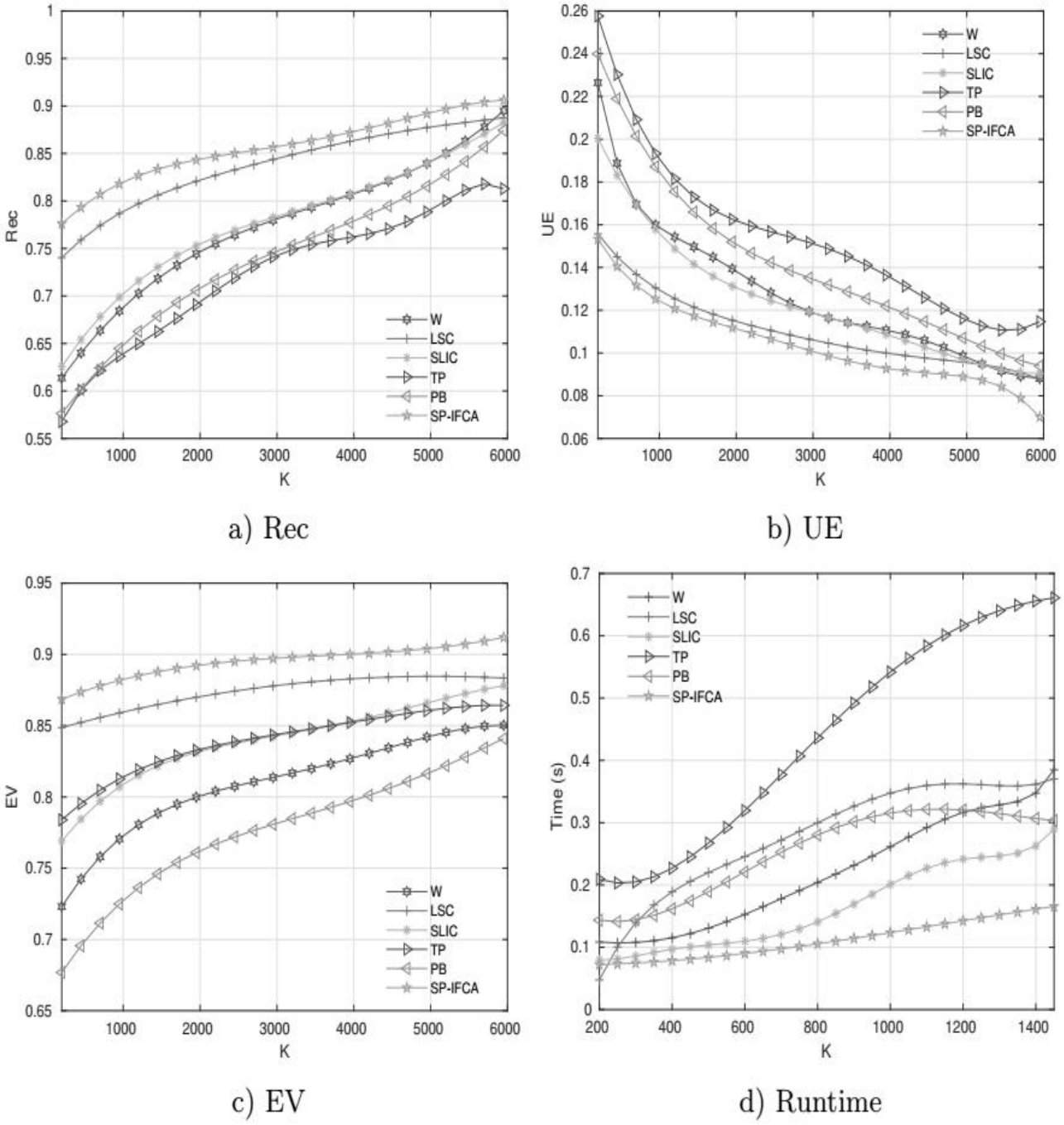

Figure 4. Average evaluation of the metrics, for the test subset of the BSDS500 database, and different K values.

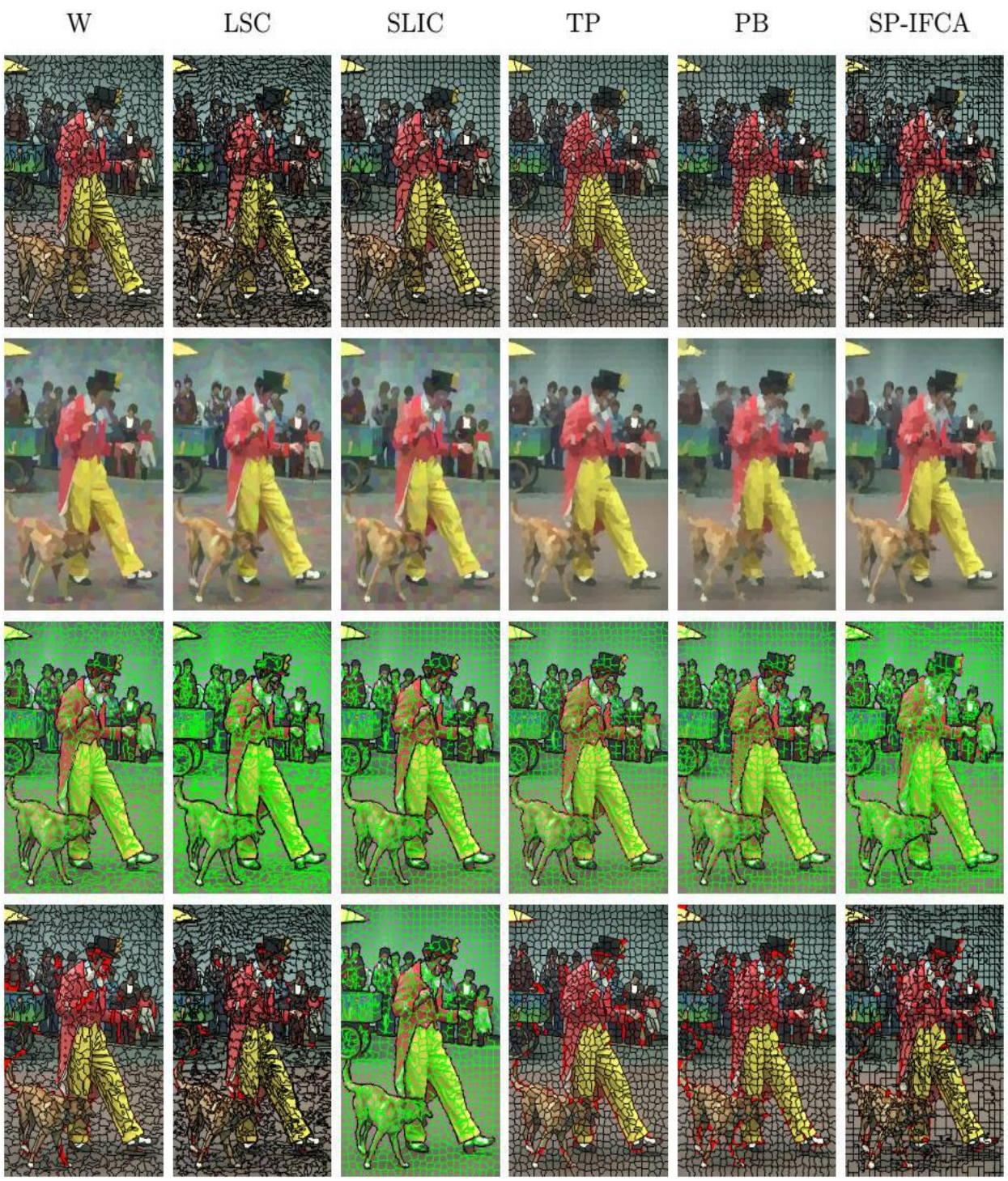

Figure 5: Visual results for the **230063** image of the ***BSDS*500** database test subset and $\boldsymbol{K = 800}$.

6. Conclusions

In this paper, an algorithm to extract superpixels in grayscale and color images was introduced, it is based on an adaptation of the $IFCM$ algorithm. The characteristics of this clustering algorithm allowed it to handle uncertainty more efficiently, resulting in a better allocation of pixels to the superpixels. The performance of the proposed algorithm against magnetic resonance images degraded with noise, allowed to obtain average values of $Rec = 0.957$, $UE = 0.059$ and $EV = 0.988$, per study, as well as all the values of K.

In contrast, for the test color images, the average values obtained were $Rec = 0.849$, $UE = 0.108$ and $EV = 0.907$, for all K values. A better performance of the proposed $SP - IFCA$ algorithm compared to comparative algorithms was demonstrated through quantitative and subjective evaluations, as well as a shorter processing time.

Future work will focus on incorporating spatial information as another feature for local clustering, as well as texture information to generate more homogeneous superpixels.

Acknowledgments

This work was supported by the Tecnológico Nacional de México/CENIDET trough the project entitled “Clasificador para detectar fibrilación auricular en señales electrocardiográficas utilizando una red recurrente profunda entrenada con momentos de tiempo-frecuencia”, as well as by CONACYT.

References

Achanta, R., Shaji, A., Smith, K., Lucchi, A., Fua, P., & Süsstrunk, S. (2010). Slic superpixels. *Ecole Polytechnique Fédéral de Lausssanne* (EPFL). *Tech. Rep, 149300* :155–162.

Arbelaez, P., Maire, M., Fowlkes, C., & Malik, J. (2011). Contour detection and hierarchical image segmentation. *IEEE Trans. Pattern Anal. Mach. Intell., 33*(5), 898–916. http://doi.org/10.1109/TPAMI.2010.161

Atanassov, K. T. (2017). Intuitionistic fuzzy logics. *Studies in Fuzziness and Soft Computing*. *351*.Springer. https://doi.org/10.1007/978-3-319-48953-7

Buyssens, P., Gardin, I., Ruan, S., & Elmoataz, A. (2014). Eikonal-based region growing for efficient clustering. *Image and Vision Computing*, *32*(12), 1045-1054. https://doi.org/10.1016/j.imavis.2014.10.002

Chaira, T. (2015). Medical image processing: *Advanced fuzzy set theoretic techniques*. CRC Press.

Felzenszwalb, P. F., & Huttenlocher, D. P. (2004). Efficient graph-based image segmentation. *International Journal of Computer Vision, 59*(2), 167-181. https://doi.org/10.1023/B:VISI.0000022288.19776.77

Hu, Z., Zou, Q., & Li, Q. (2015). Watershed superpixel. In *2015 IEEE International Conference on Image Processing (ICIP)*(pp. 349-353). https://doi.org/10.1109/ICIP.2015.7350818

Humayun, A., Li, F., & Rehg, J. M. (2015). The middle child problem: Revisiting parametric min-cut and seeds for object proposals. In *Proceedings of the IEEE International Conference on Computer Vision* (pp. 1600-1608).

Levinshtein, A., Stere, A., Kutulakos, K. N., Fleet, D. J., Dickinson, S. J., & Siddiqi, K. (2009). Turbopixels: Fast superpixels using geometric flows. *IEEE transactions on pattern analysis and machine intelligence*, *31*(12), 2290-2297. https://doi.org/10.1109/TPAMI.2009.96

Li, Z., & Chen, J. (2015). Superpixel segmentation using linear spectral clustering. In *Proceedings of the IEEE Conference on Computer Vision and Pattern Recognition* (pp. 1356-1363).

Machairas, V., Decencière, E., & Walter, T. (2014). Waterpixels: Superpixels based on the watershed transformation. In *2014 IEEE International Conference on Image Processing (ICIP)* (pp. 4343-4347). IEEE. https://doi.org/10.1109/ICIP.2014.7025882

Martin, D. R., Fowlkes, C. C., & Malik, J. (2004). Learning to detect natural image boundaries using local brightness, color, and texture cues. *IEEE transactions on pattern analysis and machine intelligence*, *26*(5), 530-549. https://doi.org/10.1109/TPAMI.2004.1273918

Moore, A. P., Prince, S. J., Warrell, J., Mohammed, U., & Jones, G. (2008, June). Superpixel lattices. In *2008 IEEE conference on computer vision and pattern recognition* (pp. 1-8). IEEE. https://doi.org/10.1109/CVPR.2008.4587471

Neubert, P., & Protzel, P. (2014). Compact watershed and preemptive SLIC: On improving trade-offs of superpixel segmentation algorithms. In *2014 22nd international conference on pattern recognition* (pp. 996-1001). IEEE. https://doi.org/10.1109/ICPR.2014.181

Pătraşcu, V. (2007). Fuzzy image segmentation based on triangular function and its n-dimensional extension. In *Soft Computing in Image Processing* (pp. 187-207). https://doi.org/10.1007/978-3-540-38233-1_7

Shi, J., & Malik, J. (2000). Normalized cuts and image segmentation. *IEEE Transactions on pattern analysis and machine intelligence*, *22*(8), 888-905. https://doi.org/10.1109/34.868688

Stutz, D., Hermans, A., & Leibe, B. (2018). Superpixels: An evaluation of the state-of-the-art. *Computer Vision and Image Understanding*, *166*, 1-27. https://doi.org/10.1016/j.cviu.2017.03.007

Szmidt, E. (2014). *Distances and similarities in intuitionistic fuzzy sets* (Vol. 307). Switzerland: Springer International Publishing.

Web, B. (2004). Simulated brain database. McConnell Brain Imaging Centre, Montreal Neurological Institute, McGill.

Xu, Z. (2013). *Intuitionistic fuzzy aggregation and clustering* (Vol. 279). Springer.

Yao, J., Boben, M., Fidler, S., & Urtasun, R. (2015). Real-time coarse-to-fine topologically preserving segmentation. In *Proceedings of the IEEE conference on computer vision and pattern recognition* (pp. 2947-2955).

Zhang, Y., Hartley, R., Mashford, J., & Burn, S. (2011). Superpixels via pseudo-boolean optimization. In *2011 International Conference on Computer Vision* (pp. 1387-1394). https://doi.org/10.1109/ICCV.2011.6126393